Characterization of austempered ductile iron through Barkhausen noise measurements

Christine d'Amato, Catherine Verdu, Xavier Kleber, Gilles Regheere, Alain Vincent

Characterization of Austempered Ductile Iron Through Barkhausen Noise Measurements

C. D'Amato,[1,2] C. Verdu,[1] X. Kleber,[1] G. Regheere[1,2] and A. Vincent[1,3]

The outstanding mechanical properties of austempered ductile irons (ADI) are linked to the microstructure of the matrix obtained by subjecting a ductile iron with an appropriate compo-sition to a heat treatment called austempering. Then the microstructure of the matrix consists of bainitic ferrite with different volume fractions of retained austenite. The aim of this work is to use the magnetic Barkhausen noise (MBN) as a nondestructive method for characterizing the microstructure of ADI. First, it is shown that the amplitude and position of the peak-shaped MBN response is quite sensitive to the microstructure of the matrix of ductile irons. Thus each type of constituent (equiaxial ferrite, pearlite, martensite or bainite) exhibits a typical response and, in turn, it can be identified from the MBN response. Furthermore, a good correlation is found between MBN signal parameters and ADI heat treatment parameters, indicating that MBN is also quite sensitive to fine evolutions of the microstructure of ADI. MBN peak position is especially sensitive to the type of bainite, whereas peak amplitude is linked to the progress of the bainite reaction. Hence MBN measurements appear to be a powerful tool to assess some important microstructural features of ADI castings.

KEY WORDS: SG ductile iron; austempered ductile iron; bainite; magnetic Barkhausen noise.

1. INTRODUCTION

Austempered ductile irons (ADI) offer attractive combinations of mechanical and service properties (toughness and ductility associated with high strength and wear resistance). These properties are the result of the mixture of phases that is obtained through the manufacturing process: casting, austenitization, and austempering. The microstructure mainly consists of graphite nodules embedded in a so-called bainitic matrix, in which fine laths or plates of ferrite and retained austenite are tightly imbricated. A large variety of bainitic structures can be obtained by varying composition and heat treatment parameters, and, in turn, the properties mentioned above are tightly linked to the good achievement of the manufacturing process. Hence there is a great demand from foundries to develop nondestructive characterization techniques that would enable one to assess the quality of the product.

In the past, several methods of nondestructive evaluation have been tested on ADI. Ultrasonic velocity[1,2] is sensitive to both the nodularity of graphite and the bainitic matrix structure. However, it seems that ultrasonic methods are more appropriate to characterize the nodularity of graphite. Eddy-current and classical magnetic methods[3,4] also have been proposed. Good correlation has been found between retained austenite content and eddy currents parameters, for example.

[1] Groupe d'Etudes de Metallurgie Physique et de Physique des Matériaux-UMR CNRS 5510, Institut National des Sciences Appliquées, 69621 Villeurbanne Cedex, France.
[2] CTIF, 44 av. de la Division Leclerc, 92312 Sèvres cedex, France.
[3] E-mail: Alain.Vincent@insa-lyon.fr

However, all these methods provide a macroscopic physical quantity averaged over the various phases present in the material, which makes it difficult to analyze the contribution of each phase. In contrast, the magnetic Barkhausen noise (MBN), which occurs during the magnetization process of a material, originates almost directly from the ferromagnetic phases in this material. Moreover, MBN features are tightly linked to the microstructure of these ferromagnetic phases. Therefore MBN could provide valuable information about the good achievement of the manufacturing process of ADI. Although many works have been reported in the literature dealing with the relation between the MBN and microstructural constituents in steels (ferrite, pearlite, martensite),[5–7] to our knowledge nothing is available concerning MBN in ADI. Hence the objective of the current work is to investigate the main features of MBN in spheroidal graphite cast iron (SGCI), placing emphasis on the bainite reaction in ADI. For that purpose, on the one hand, different SGCI were prepared with different single constituents (ferrite, pearlite, martensite, or bainite), in order to compare the MBN features of these matrix constituents. On the other hand, series of specimens were austempered for increasing time and at different temperatures to study the sensitivity of the MBN to the progress of the bainite reaction.

In this paper, first, the SGCIs investigated in the present work are presented. In the following part, the MBN characteristics of these materials are reported. In the last part of the paper, the MBN results are discussed in relation to the main microstructural features of the materials.

2. MATERIALS

2.1. Background on Austempered Ductile Irons

The manufacturing conditions and properties of ADI have been reviewed by several authors (e.g., see[8,9]). First, as-cast ductile irons are fully austenitized in the temperature range 850°C–950°C. Then they are rapidly cooled to the temperature range suitable for bainite reaction. Austempering consists of an isothermal holding in the temperature range 250°C–450°C for typically 0.5–2 h before cooling to room temperature.

During austempering, bainitic ferrite nucleates and grows into the austenite. The high silicon content (>2%) of ductile irons hinders the precipitation of carbides during the transformation. Moreover, carbon diffuses from the supersaturated ferrite into the surrounding austenite. Consequently, the nontransformed austenite is gradually stabilized, allowing it to be finally retained when the material is cooled to room temperature. However, long austempering time leads to the decomposition of austenite into ferrite and carbide, which is quite harmful for mechanical properties (loss in ductility and toughness).

Hence the austempering process is usually divided in two main stages: stage I: $\gamma \rightarrow \alpha + \gamma_r$; stage II: $\gamma_r \rightarrow \alpha +$ carbides. The period between the end of stage I and the beginning of stage II is referred to as the "process window" and corresponds to highest retained austenite contents and the best mechanical properties (maximum of the toughness). To obtain a wider process window, alloying elements, such as Mo, Ni, Mn, or Cu, which delay the both stages of the bainite reaction, are added.

Bainitic ferrite morphology gradually evolves with austempering temperature. Two types of ADI are usually distinguished. At temperatures below 330°C or so, ferrite units look like fine needles or laths and the microstructure is called "lower bainite." At temperatures above 330°C or so, the microstructure consists of coarser ferrite plates arranged in sheaves and is referred to as "upper bainite."

2.2. Test Samples

In this study, SGCI with three different chemical compositions (nonalloyed, mid alloyed, and alloyed, hereafter noted C1, C2, C3, respectively) were cast (see Table I). Cylinders with 20-mm diameter were machined and heat-treated. Inert atmosphere was used to avoid decarburization. To simulate the occurrence of inappropriate heat treatment conditions, a specific sample was treated without such care, leading to some surface decarburization.

On the one hand, it was necessary to characterize the specific MBN characteristics of each constituent that can be found in ADI. Therefore five different SGCI samples with different matrix constituents were first manufactured. Equiaxial ferrite, pearlite, martensite, and lower and upper bainite were obtained according to the heat treatment parameters presented in Table II.

Table I. Chemical Compositions of the Different SGCIs Investigated (in wt%)

	C	Si	Mn	S,P	Mg	Cu	Ni	Mo
C1	3.6	2.4	0.2	<0.02	0.04	0.02	0	0
C2	3.6	2.4	0.2	<0.02	0.04	0.7	0.5	0
C3	3.6	2.4	0.2	<0.02	0.04	0.7	0.5	0.2

Table II. Heat Treatment Conditions for SGCI Samples with Different Matrix Constituents

Matrix	Composition	heat treatment
Ferrite	C1	Austenitization 900°C for 3 h cooling: 50°C/h ⇒800°C; 20°C/h ⇒600°C; air cooling
pearlite	C1	Austenitization 900°C for 2 h cooling: 50°C/h ⇒850°C; blowing air cooling
martensite	C2	Austenitization 900°C for 2 h cooling: 50°C/h ⇒850°C; oil quench
upper bainite	C2	Austenitization 850°C for 1.5 h Austempering: 375°C for 0.5 h, air cooling
lower bainite	C2	Austenitization: 850°C for 1.5 h Austempering: 280°C for 0.5 h, air cooling

On the other hand, series of ADI samples were also realized divided in two compositions, C1 and C3, and different heat-treatments: austenitization temperatures 850°C and 900°C for 1.5 h, austempering temperatures 280°C, 350°C, 375°C, and 425°C for different austempering times ranging from 0.25 h to 8 h, so as to obtain a wide range of microstructures. The austenitization time was chosen long enough to obtain a complete homogenization of the matrix. For each set of heat treatment conditions and composition of ADI, two samples were prepared to evaluate the reproducibility of the preparation and measurement procedures. All ADI specimens of a given composition were prepared from the same casting, which means the graphite nodularity and volume fraction were identical for all these samples.

2.3. Microstructural Characterization

Microstructural characterization has been performed on pieces cut from the end of the cylinders. Several methods have been used to verify the matrix microstructure of the samples. Optical and scanning electron microscopy observations have been realized after polishing and etching with 4% Nital. Optical microscopy enables us to verify that the expected microstructures have been obtained for the constituents of the SGCI samples (Fig. 1 a–e). It reveals that for the sample heat-treated without taking care of heat treatment conditions, the core microstructure is actually martensitic, whereas a layer of ferrite is present at the surface (Fig. 1 f).

For the series of ADI samples, the fine evolution of the bainitic matrix with the heat treatment parameters also has been studied. In Figure 2, scanning electron micrographies show, as expected, that the bainitic microstructure becomes coarser with increasing austempering temperature.

To quantify the progress of the bainite reaction, X-ray diffraction measurements have been performed on the polished surface with a SIEMENS diffractometer equiped with a Co target. Retained austenite volume fraction is calculated using the ratio between several diffraction peaks of ferrite (200, 211, 220) and austenite (200, 220, 311, 222).

No significant amount of martensite is detected on the spectra for all the treatment conditions of the present work. Furthermore, as illustrated for some conditions in Figure 3, retained austenite volume fraction never significantly increases with increasing austempering time. This result suggests that the samples never stand in the first stage of the bainite reaction. Moreover, most of the samples present no significant variation of the retained austenite volume fraction with austempering time, as illustrated in Figure 3 for samples austenitized at 850°C and austempered at 350°C. It indicates that they are situated within the process window. However, a drop of the retained austenite volume fraction is observed for samples austempered at 425°C for long time. It indicates that the stage II of the bainite reaction has been reached (Fig. 3).

The delaying effect of the alloying elements is also clearly illustrated in Figure 3 by these samples austenitized at 850°C and austempered at 425°C. For composition C1, retained austenite content drops after 0.25 h and stage II is almost finished after 1 h, whereas for composition C3, the retained austenite content only begins to drop after 1 h.

3. MAGNETIC BARKHAUSEN NOISE MEASUREMENTS

3.1. Experimental Conditions for MBN Measurements

The apparatus for measuring MBN in this work is presented in Figure 4. A magnetic circuit, a U-shaped core made of a high permeability iron-nickel alloy closed through the cylindrical samples, is magnetizd by means

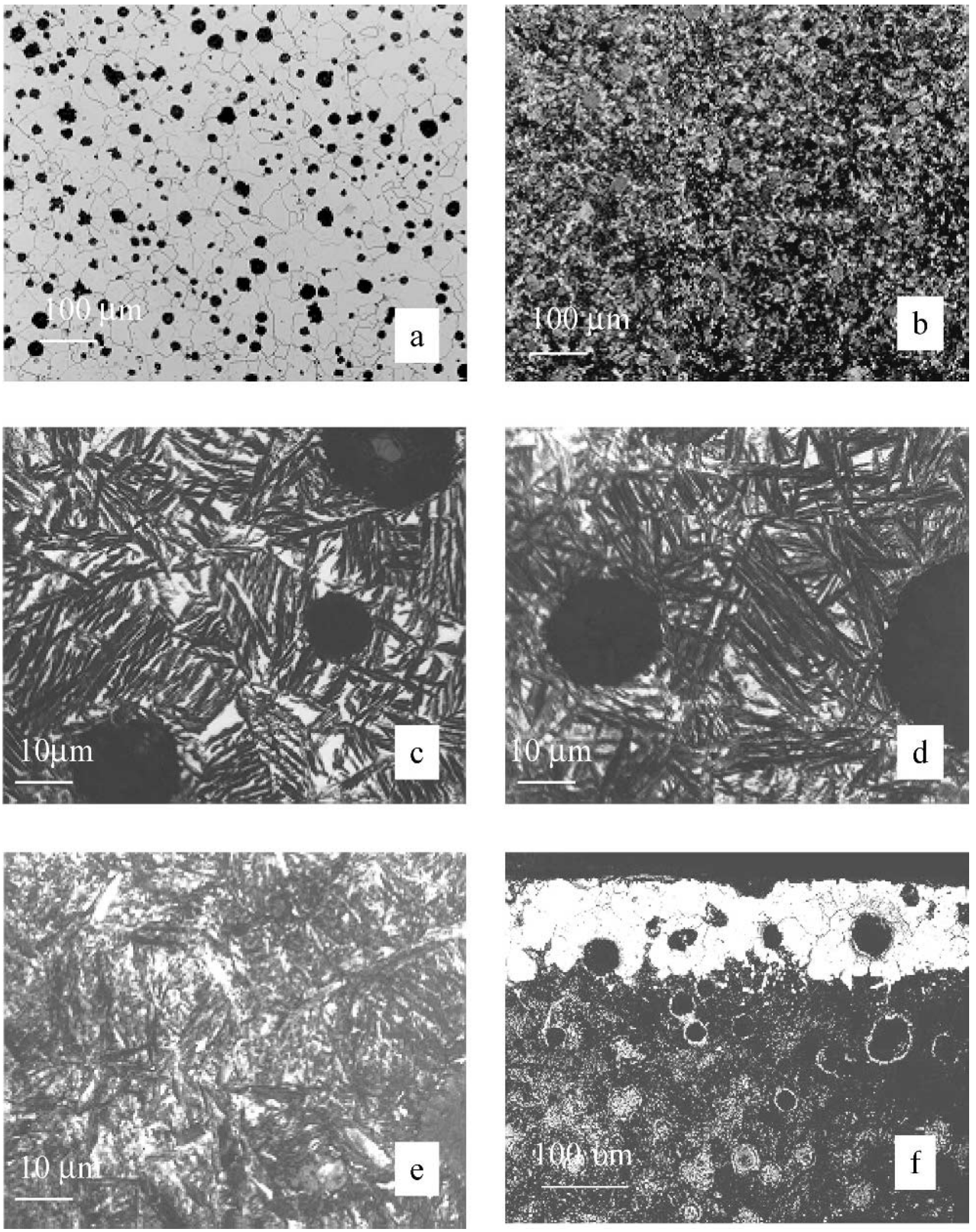

Fig. 1. Light micrographs of test samples with different matrix constituents. (a) equiaxial ferrite, (b) pearlite, (c) upper bainite, (d) lower bainite, (e) martensite, (f) martensite with decarburization layer of ferrite.

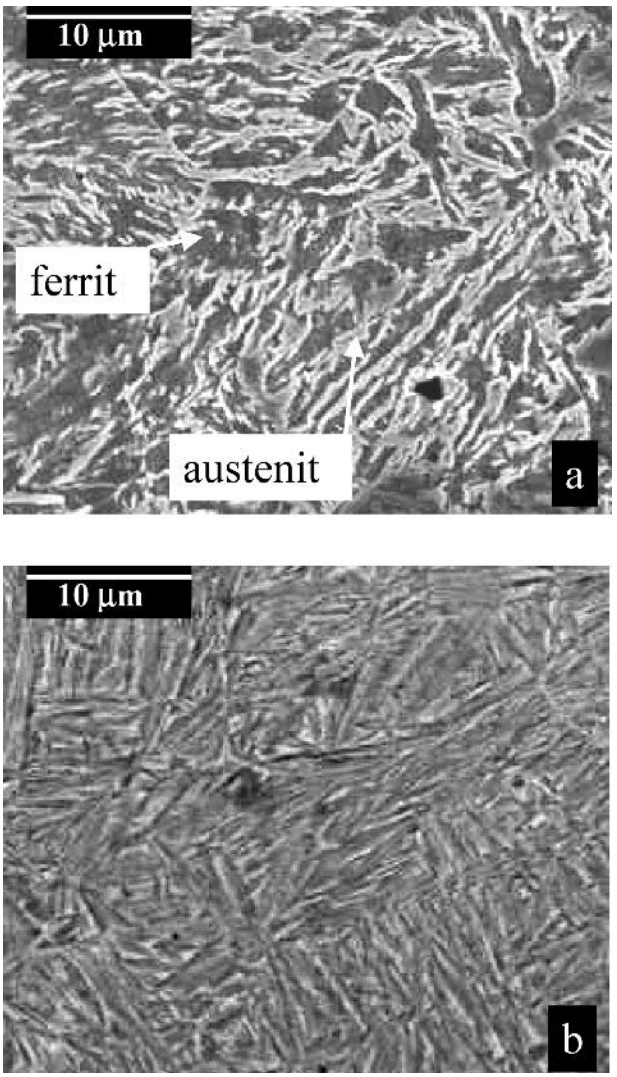

Fig. 2. Scanning electron micrographs of the (a) upper and (b) lower bainite microstructures (samples austempered at 425° and 280°C, respectively).

of a coil wound around the U-shaped core. The magnetic field H induced in the samples is measured at its surface by a Hall sensor. The samples are magnetized from saturation to saturation with a quasi-triangular waveform. The corresponding magnetization rate is $|dH/dt| \cong 6\ kAm^{-1}s^{-1}$.

The electromagnetic signals are detected using a surrounding coil probe. Following a preamplification stage (gain, 25), MBN is selected from the overall signal through a high-pass filter (cut-off frequency, 2 kHz). Then, following a second amplification stage (gain, 100), the instant[1] root mean square value of the noise

[1] The integration time of the RMS circuit was fixed to 25 ms for every measurement.

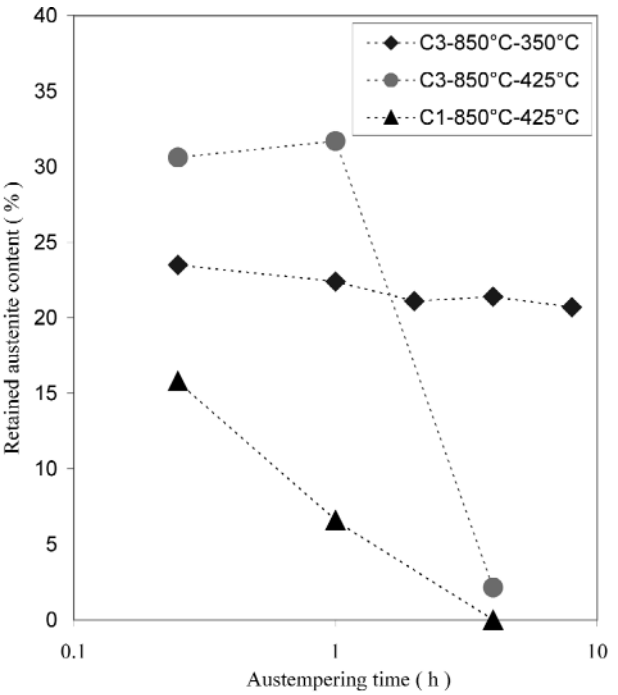

Fig. 3. Volume fraction of retained austenite, obtained from x-ray diffraction measurements, versus austempering time, for different compositions and austempering temperatures.

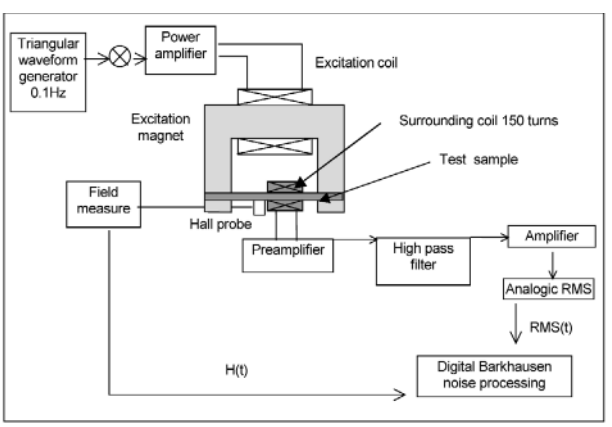

Fig. 4. Schematic diagram of MBN apparatus.

voltage, hereafter noted V_{RMS}, is delivered. Because the variation of V_{RMS} versus H, hereafter called MBN response or $V_{RMS} = f(H)$ response, is symmetric for increasing and decreasing H, only the part of the response at increasing H is presented in what follows. Furthermore, the MBN response is always peak shaped and is characterized by simple parameters: the maximum amplitude of the peak,[2] V_M, and the corresponding

[2] The background noise (V_N) is subtracted from the total noise according to $V_M = \sqrt{(V_{RMS}^2 - V_N^2)}$.

magnetic field, hereafter called peak position, H_M. The typical scatter for several measurements on the same ADI specimen was found to be ± 0.05 V and ± 0.5 kA/m for V_M, and H_M, respectively. Finally, it should be mentioned that the difference between the measured values for twin samples never exceeded 5%, which testifies of the good reproducibility of the preparation procedure and MBN measurements.

3.2. Experimental Results

3.2.1. MBN from SGCI with Different Matrix Constituents

Figure 5a and b shows the MBN response obtained for the SGCI prepared with different matrix constituents: equixial ferrite, pearlite, martensite, and upper and lower bainites. It is worth noting that MBN responses vary to a large extent with the matrix microstructure. SGCI with ferrite or pearlite (Fig. 5a) exhibits a very high peak appearing at low magnetic field, $H_M \cong 0.2$ and 1 kA/m, respectively. In contrast, SGCI with martensite or bainite (Fig. 5a and b) exhibits a much smaller peak, whose amplitude is about 10 times or so smaller than that of SGCI with ferrite or pearlite. In addition, these peaks appear at higher fields (H_M ranging from 2 to 3.6 kA/m). Furthermore, it can be seen (Fig. 5b) that the peak of SGCI with upper bainite appears at a lower field than that of SGCI with lower bainite. This point is studied in more detail in Section 3.2.2.

The specific response of the sample presenting a decarburized layer (with ferrite in this layer and martensite in the core) is shown in Figure 6. In this case, the MBN response exhibits two well-separated peaks. The field positions of these peaks, $H_M \cong 0.3$ and 3.4 kA/m, are close to those of the peaks observed for the ferritic and martensitic matrices, respectively. Therefore the low field peak and the high field peak can be ascribed to the decarburized layer and the core matrix, respectively.

3.2.2. Influence of Heat Treatment Conditions on MBN from ADI

The influence of heat treatment parameters on the MBN response of ADI samples has been investigated according to the experimental conditions defined in Section 2. As illustrated previously, this MBN response is usually peak shaped. However, it should be mentioned that for particular heat treatment conditions, especially for some samples austempered at 280°C or 350°C, the response exhibits a secondary maximum,

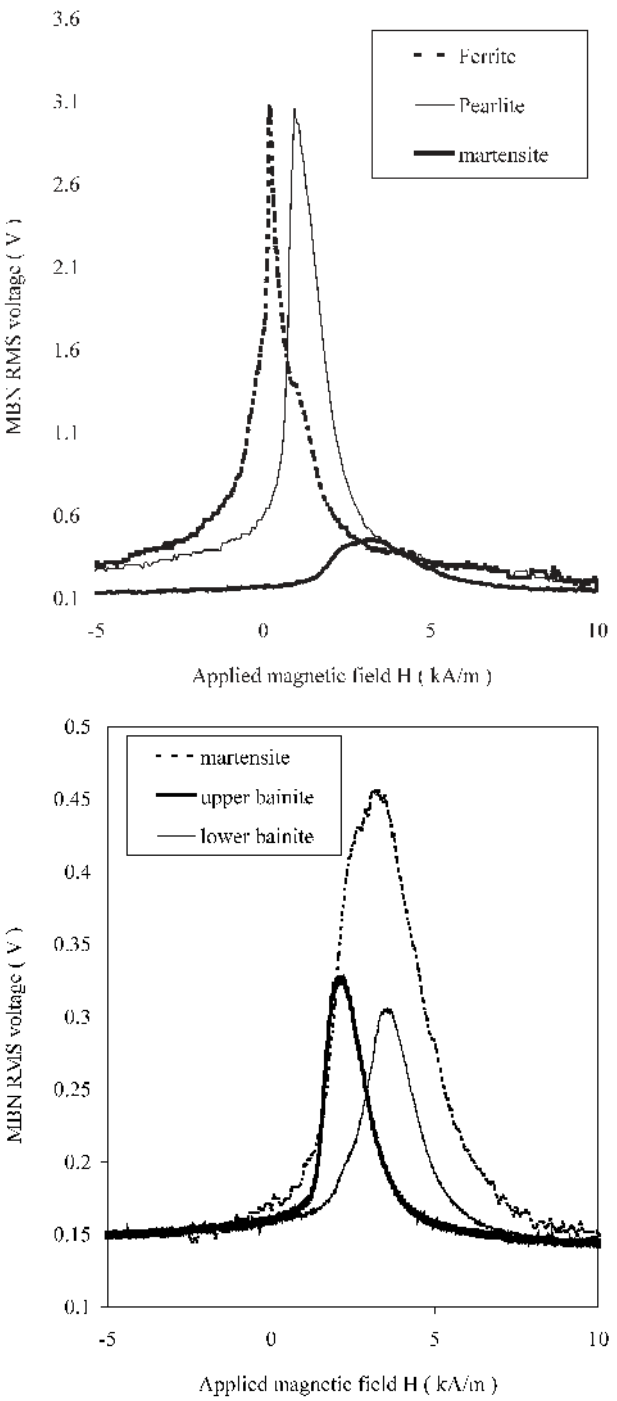

Fig. 5. $V_{RMS} = f(H)$ responses for SGCI samples with different matrix constituents: (a) equiaxial ferrite, pearlite, and martensite; (b) martensite, upper and lower bainite.

as is illustrated in Figure 7 for a C1 sample. Such a secondary peak seems to be clearly distinguishable only for particular heat treatment conditions. For example, it can be seen in Figure 7 that this peak vanishes only

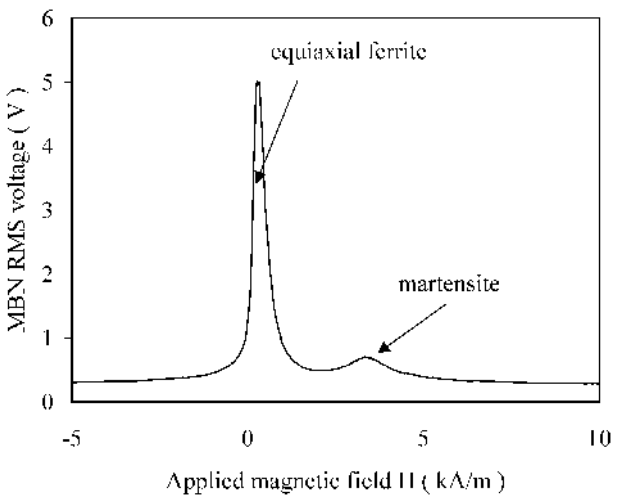

Fig. 6. V_{RMS} = f(H) for martensitic SGCI sample with a decarburized layer.

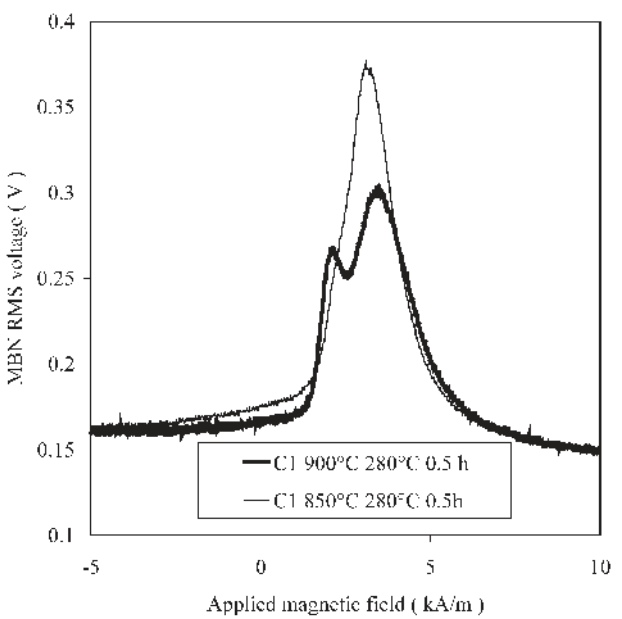

Fig. 7. Example of influence of the austenitization temperature on the substructure of the V_{RMS} = f(H) responses: samples of composition C1 austempered at 280°C for 0.5 h.

by changing the austenitization temperature from 850°C to 900°C, the austempering conditions being the same. Furthermore, it should be mentioned that such a secondary peak cannot be ascribed to equiaxial ferrite or pearlite which produces MBN for much lower magnetic fields than that corresponding to this secondary peak. Yet, further investigations are necessary to describe the detailed properties of this secondary peak, and in this work, only the characteristics of the high field peak (the main peak in Fig. 7) are reported.

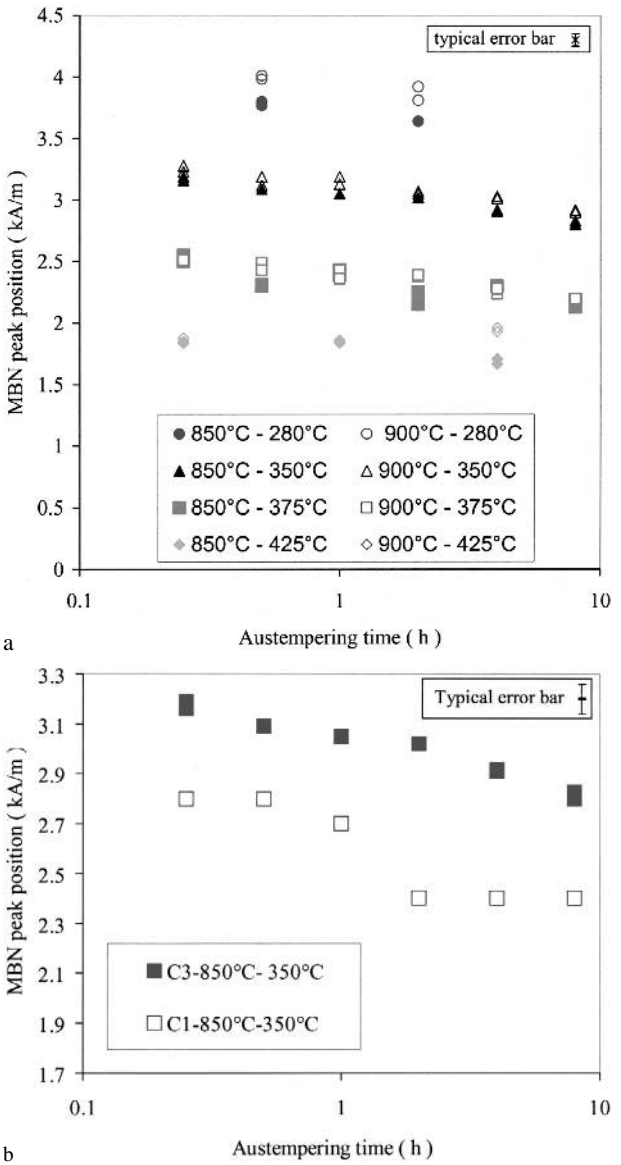

Fig. 8. MBN peak position H_M versus austempering time: (a) influence of austenitization and austempering temperatures for C3 composition. (b) influence of composition for samples austenitized at 850°C and austempered at 350°C (data are plotted for both samples of each twin pair; when only one data point is distinguishable, this means that the two measures are equal).

Field position H_M of the MBN Peak. Figure 8 a shows H_M values versus austempering time for every C3 sample. From this set of data, it appears that the main influencing parameter for the field position of the MBN peak is austempering temperature. The peak position range decreases from 4 – 3.6 kA/m to 2 – 1.7 kA/m as austempering temperature is increased from 280°C to 425°C. The other heat treatment parameters influence H_M weakly. Thus H_M tends to decrease when austempering

time is increased. For many conditions H_M seems to increase, but only slightly, with increasing austenitization temperature.

The same tendencies were observed for composition C1, but the field range corresponding to each austempering temperature is slightly shifted toward lower fields with decreasing the content of alloying elements. This shift is illustrated in Figure 8b for C1 and C3 samples austenitized at 850°C and austempered at 350°C.

Maximum Amplitude V_M of the MBN Peak. The maximum amplitude of the peak also varies with heat treatment parameters. In contrast with what was observed for H_M, the austempering time is an important influencing parameter for V_M. Thus Figure 9a shows that for C3 composition a gradual increase of V_M is observed with increasing austempering time for low austempering temperatures (280, 350, and 375°C). This increase of V_M with increasing austempering time is much more important for the highest austempering temperature (425°C). This stage of steep increase of V_M for samples austempered at 425°C occurs earlier for composition C1 than for composition C3, as illustrated in Figure 9b.

Finally, the influence of austenitization temperature on V_M evolution versus austempering time is illustrated in Figure 10 for C3 composition: the evolutions of V_M seem to be parallel, but for a given austempering time V_M is lower for the samples austenitized at 900°C than for those austenitized at 850°C.

4. DISCUSSION

4.1. Background on MBN

When a ferromagnetic material is subjected to a magnetic field, it tends to become magnetized, which is usually observed at a macroscopic scale, for instance by recording the hysteresis loop B = f(H).[3] In fact, this occurs through the reorganization of the magnetic microstructure made of magnetic domains at a mesoscopic scale (Weiss domains). Among the various mechanisms involved in this complex process, it is well known that irreversible creations and motions of domain walls are responsible of the MBN.[10,11] Thus MBN is representative of the microdynamics of the reorganization process, while the macroscopic magnetization and the associated B = f(H) loop represent the instant cumulation of all the elementary events. However, from the common origin of the B = f(H) loop and the MBN, it

[3] B = magnetic flux density.

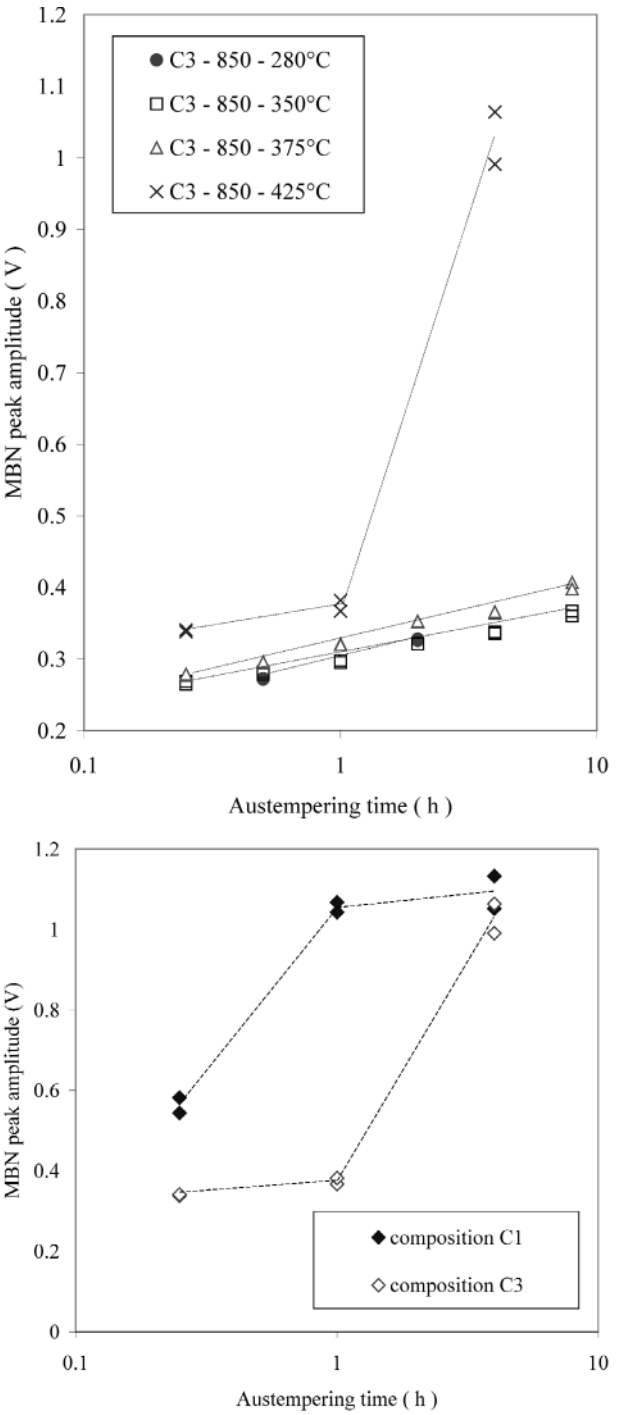

Fig. 9. MBN peak amplitude V_M versus austempering time: (a) influence of austempering temperature for C3 composition austenitized at 850°C; (b) influence of composition for samples austenitized at 850°C and austempered at 425°C (data are plotted for both samples of each twin pair: when only one data point is distinguishable, this means that the two measures are equal).

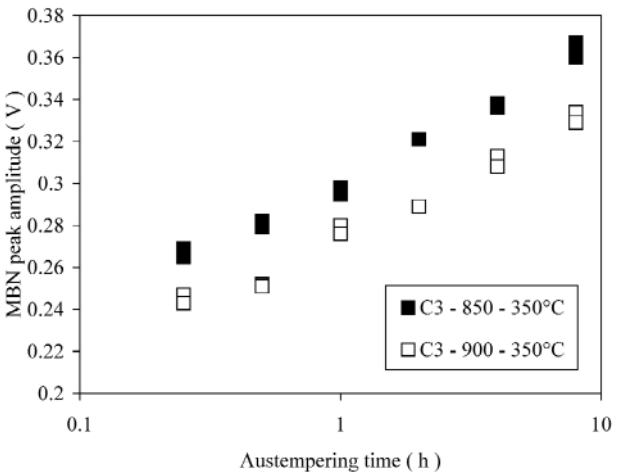

Fig. 10. MBN peak amplitude V_M versus austempering time: influence of austenitization temperature for C3 composition austempered at 350°C.

results that a few macroscopic magnetic properties and MBN features are related. For instance, the coercive field in the hysteresis cycle is generally in the field range of the MBN peak, because both field ranges correspond to an intense reorganization of the magnetic microstructure. As a matter of fact, the characteristics of MBN are tightly linked with those of the domain wall mechanisms. That is, the field position of the peak, as well as the coercive field, generally increase from soft to hard magnetic materials.[12,13] This arises from several microstructural mechanisms. First, domain wall creation is more difficult as the grain size is decreased (because of an unfavorable balance between wall energy and magnetostatic energy in the material). Second, the wall motions require higher fields as pinning sites, such as second-phase precipitates, dislocation tangles, or grain boundaries are more numerous. Furthermore, the distortion of the crystalline network as a result of ordered interstitial atoms as in tetragonal martensite, which are responsible for a single easy magnetic axis,[14] also makes the magnetic microstructure reorganization harder. Finally, it should be mentioned that the presence of non magnetic phases in a ferromagnetic material (such as graphite nodules and austenite in SGCI) is responsible for internal demagnetizing fields opposing the applied field.

The amplitude of the MBN is more complex to describe because it depends not only on the dynamics of motion of domain walls between pinning places, but also on the transfer function of the encircling coil and receiver that detect the MBN electromagnetic signals.[6] As a result of this complexity, in this work our results concerning the MBN amplitude will mainly be discussed by comparison with similar influence reported in the literature.

MBN may be also influenced by stress, being applied or internal. This dependence of MBN upon stress is caused by the preferred domain orientations that are induced because of the effect of magnetostriction. For crystalline structures with a positive magnetostriction, such as α-ferrite or α′-martensite, a tensile stress favors the domains magnetized in directions closest to the stress axis to grow at the expense of the others, thus reducing the magnetoelastic energy. As a result, when MBN is measured with a magnetization direction parallel to the stress axis, an increase of the MBN peak height is generally observed with increasing tensile stress and conversely for a compressive stress.[15] In contrast, few data are available for magnetization directions nonparallel to the stress axis. Concerning the present work, only internal stresses of type I, often called macroresidual stresses (RS), or internal stresses of type II, also called microresidual stresses, might interfere with the microstructure influence on the MBN. Macro-RS may result from a different strain history between surface and core of a part or specimen (during cooling). They are expected to be low in our specimens, because of their small size. Moreover, it has been shown elsewhere[16] that for ADI the influence of a macrostress on MBN remains weak in comparison with that of the microstructure state. Micro-RS, as well as a high dislocation density, are inherent to the martensitic or bainitic transformations. They occur because of the mismatch between the transformation strain linked with the crystallographic structure change of one crystal with respect to its neighbors or the surrounding matrix. As for the aforementioned tetragonal distortion, micro-RS locally favor specific magnetic orientations, and hence their average effect on MBN is expected to be similar to that of tetragonal distortion.

4.2. MBN from SGCI in Relation to the Matrix Constituent

The MBN responses obtained for SGCI with ferritic, pearlitic, and martensitic matrices look like those obtained for ferritic, pearlitic, and martensitic steels, respectively,[6] both in terms of field position H_M and of the relative maximum amplitude of the peaks. So, despite the nonmagnetic graphite nodules that are expected to have a local influence on the magnetic microstructure of the surrounding matrix, the MBN response is not too much modified. Especially, the close positions of the peaks in steel and SGCI for similar

matrix constituents can be explained by the fact that the average demagnetizing field in SGCI remains low in the MBN peak range, where the macroscopic magnetization of the material is also low. So, the presence of nonmagnetic spheroidal graphite in SGCI only seems to influence the intensity of the MBN response from the matrix, which is expected to be reduced in proportion of the volume fraction of graphite. Thus each microstructural constituent exhibits its own MBN activity represented by a typical peak-shaped response. As a matter of fact, we can observe great differences in term of peak field position and peak height.

Compared to ferrite, the high magnetic hardness of martensite is usually explained by its very fine microstructure, the tetragonal distortion of the crystalline network by carbon atoms in α'-martensite, the high level of micro-RS and the high density of dislocations.[6,7] The same arguments also apply for the high field position of the MBN peak in bainitic SGCI compared to that in ferritic SGCI, because the grain size for equiaxial ferrite in SGCI samples was about 0.1 mm, whereas bainite units are about 100 times smaller. Furthermore, the bainitic α phase exhibits some tetragonality,[17] although it is less marked than that of α' martensite. Finally, the intermediate peak field position for pearlite has been already explained by the presence of cementite lamella in this constituent, which makes more difficult the reorganization of the magnetic microstructure in the neighboring ferrite lamellae.[18] Concerning the amplitude of MBN activity in martensite, various arguments have been proposed[6] to explain the low activity compared to ferrite (or pearlite): (i) due to the very fine crystalline microstructure the Barkhausen events are small (small volume swept by a wall between two pinning sites); (ii) accordingly, as shown in reference,[6] the frequency range of the electromagnetic signals emitted by martensitic microstructures is higher than that from equiaxial ferrite, and hence the encircling coil probe and receiver could be less sensitive in this high frequency range.

Finally, in the martensitic SGCI sample with a decarburized region of ferrite, each constituent produces its own typical response. This is possible because the thickness of the decarburized layer is thin enough ($\cong$100 μm) such that the electromagnetic waves emitted from the martensitic core are only weakly attenuated when they propagate through the ferrite layer. It should be mentioned that such a superposition of MBN signals produced by different microstructures has also been observed in surface hardened steels.[19,20] In that case they can be used to characterize the thickness of this layer.

4.3. Variation of the MBN Response in ADI

First, it should be recalled that the nodularity and volume fraction of the graphite phase are identical for all the samples of a given composition and hence its influence on the MBN does not change versus the austempering conditions. Second, from the microstructure study of ADI tested in this work, it has been confirmed that the heat treatment conditions do not correspond to the stage I of ADI austempering, that is, no significant amount of martensite is present in samples treated in such a way. That means the MBN activity in the investigated samples should be produced by the bainitic ferrite only, and hence the variations of MBN features have to be related to the variations of the bainite microstructure.

It has been observed that the field position of the MBN peak from ADI is mainly controlled by the austempering temperature, that is, H_M decreases with increasing austempering temperature, while the influence of austempering time and austenitization temperature are weaker. From the microstuctural point of view, different features of bainite are influenced by the austempering temperature. First, the tetragonality of the bainitic α phase has been observed to decrease with increasing austempering temperature.[17] The dislocation density and the micro-RS are also expected to be lowered with increasing austempering temperature. Furthermore, as shown in Section 2 (see Fig. 2), bainite units become larger with increasing the austempering temperature. As mentioned previously, such variations are expected to make the magnetic microstructure reorganization easier, which is in good accordance with the observed variations of the MBN peak position. The details of the bainite morphology (rather lath-like for lower bainite and feathery in upper bainite) are also expected to influence the MBN response. Such details could be responsible for the presence of a secondary peak in some samples austempered at 350°C (i.e., for intermediate bainite), but this question requires further investigation in order to be clarified.

When austempering time is increased MBN peak position slightly decreases, probably because of the slow evolution of ferrite units. Furthermore, for a given austempering time, H_M is higher for C3 than C1 (see Fig. 8b). This could be explained, at least partially, by a time shift in the bainite reaction that is slower in the alloyed ADI (C3).

These arguments concerning differences in microstructural features linked with heat treatment conditions are also quite consistent with the evolution of peak amplitude, although the relationship between microstructural features and measured MBN activity is

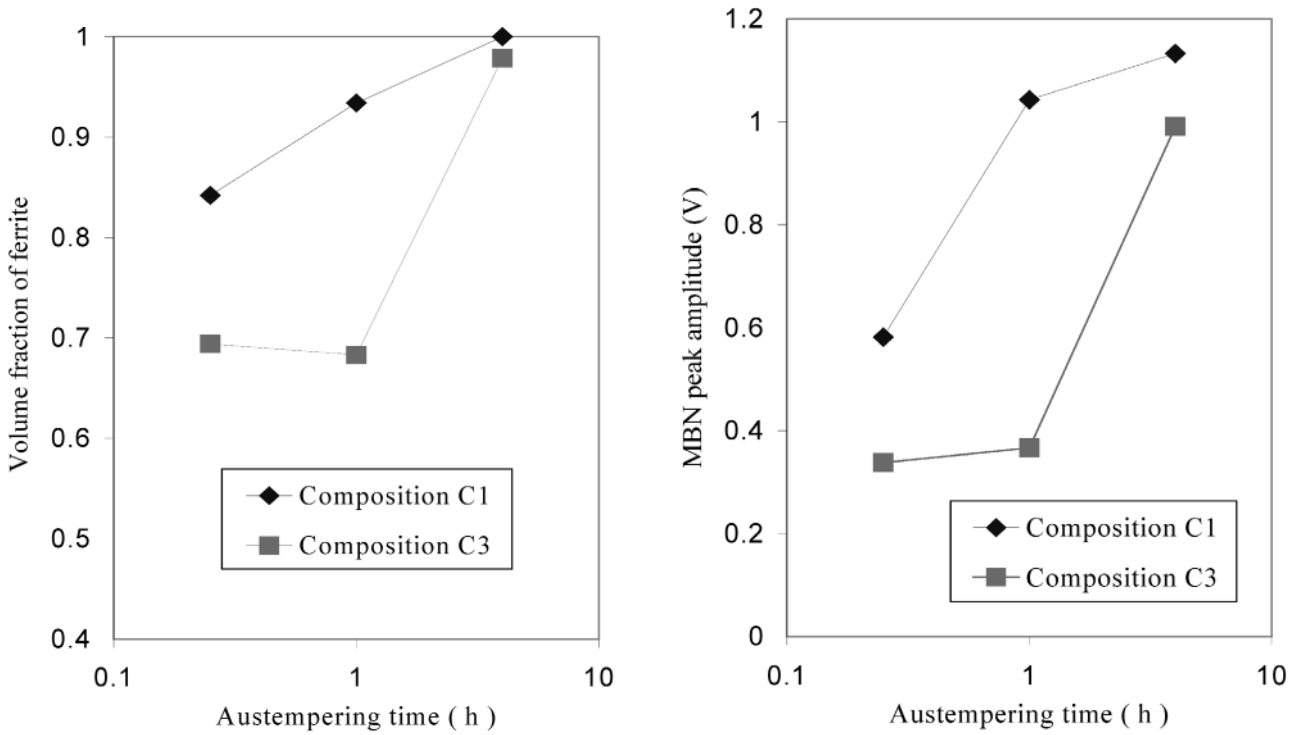

Fig. 11. Comparison between the evolutions of volume fraction of ferrite phase (a) and MBN peak amplitude (b) versus austempering time, for ADI samples of C1 and C3 compositions austenitized at 850°C and austempered at 425°C.

more complex. Thus a continual increase of V_M with increasing austempering time has been observed within the "process window," while this increase becomes much more important when stage II is reached. During the "process window" few bainitic ferrite plates continue to grow slowly, and carbon is rejected from the bainitic bainitic-ferrite into austenite, which favor MBN activity. To a certain extent, this can be compared to stages of martensite tempering, during which carbon is rejected from bainitic-martensite, which also leads to an increase in MBN activity.[6,21] When stage II is reached (during austempering at 425°C) a new mechanism has to be taken into account: the significant increase in volume fraction of bainitic-ferrite, as attested by the marked decrease of retained austenite content (see Fig. 3). That volume fraction of bainitic-ferrite is expected to influence directly the maximal amplitude of the peak, while in contrast the peak position is only weakly affected. To estimate this influence, the volume fraction of bainitic-ferrite has been plotted in Figure 11 together with V_M. Then the correlation appears clearly, but it should be noticed that the increase of V_M during stage II is far more important than a simple variation proportional to the volume fraction of the ferrite phase. Several features can contribute to this larger increase in the Barkhausen activity. The disappearance of the nonmagnetic austenite between bainite units might favor magnetic coupling phenomena between Barkhausen events generated in neighboring units, which is expected to enhance the MBN according to the Barkhausen noise theory.[22]

The comparison between different austempering temperatures is more difficult because in that case more microstructural features of bainite that influence the peak amplitude in opposite ways are changed simultaneously: tetragonality, micro-RS, morphology, and volume fraction of bainite. When austempering temperature is increased, MBN amplitude generally increases, although the retained austenite content is higher for upper bainite than for lower bainite during the "process window." This means that the major roles are then played by the tetragonality and morphology of the bainitic ferrite. Indeed, increasing the austempering temperature leads to a lower carbon content in bainite[17] and to larger bainite units (see section 2.3), which increases MBN activity.

The decrease of MBN amplitude when austenitization temperature is increased is associated with a decrease of the volume fraction of bainitic-ferrite. Yet, it is worth mentioning that, according to the interpretation of the austempering time evolution mentioned previously, the influence of austenization temperature could be as well interpreted as a delay in the bainite evolution during the process window.

Finally, the difference observed between MBN responses of samples of composition C1 and C3 could also be interpreted as a delay in the bainite evolution.

5. CONCLUSION

First of all, MBN responses of different constituents are quite different. So, the presence of unwanted constituents such as ferrite or pearlite in ADI castings can be detected because their contribution to the overall MBN response is quite different from bainitic ones.

Moreover, MBN measurements are sensitive to the fine evolutions of the metallurgical state of ADI. MBN peak parameters (position and amplitude) give complementary information to assess ADI treatment. Thus MBN peak position is very sensitive to austempering temperature, whereas the other parameters (austempering time, austenitization temperature, and composition) influence this MBN characteristic weakly. Thus upper and lower bainites can be sorted by measuring the peak position H_M. In addition, it should be mentioned that this parameter is quite valuable in evaluating the mechanical properties of ADI because yield strength of ADI varies roughly as H_M.[16] In contrast, MBN peak amplitude is especially sensitive to the progress of the isothermal reaction. An austempering time (when stage II is reached) that is too long is characterized by an important increase in the peak amplitude. The influence of the other heat treatment conditions on MBN peak amplitude is weaker. Most relationships between MBN and heat treatment conditions can be understood from the evolutions of ADI microstructural features.

Finally, it should be mentioned that some results also suggest that a detailed analysis of the substructure of the MBN response could provide additional information on the microstructural features of intermediate bainites. Such a study is in the course.

In conclusion, it has been shown that the MBN technique is potentially a very powerful tool for nondestructive characterization of ADI. The main advantage of such a technique is that the MBN signals are almost directly provided by the magnetic microstructural constituents, which enables one to identify these constituents. In comparison, for other available NDE techniques, such as those based on eddy currents, the material response results from a macroscopic average over the various constituents of the material.

However, for most practical NDE applications of MBN the principle of encircling coils could not be used. Hence, these applications require that well designed side probes are developed, capable of measuring the peak position accurately.

ACKNOWLEDGMENTS

This work was supported by the European Economic Community through a CRAFT program (BRST-CT98-5243). The EC and all the partners of the project are gratefully acknowledged.

REFERENCES

1. S. S. Lee and S. Lee, Non-destructive characterization of austempered ductile irons. *Third International Symposium of ADI*, Saarbrücken, Germany, October 3–6, 1988, pp. 533–540.
2. A. Toppuz, E. Topcu, A. Bakkaloglu, and M. Marsoglu, Microstructural investigation of austempered ductile irons with ultrasonic method, *Praktis. Metallograph.* **34**, pp. 278–287 (1997).
3. R. A. Harding, Control of the retained austenite content of ADI, 1991 World Conference on ADI. March 12–14, 1991, (Bloomingdale IL, pp. 2.2–3.1).
4. T. Ueno, M. Suenaga, Y. Ishihara, and E. Nakano, Material evaluation of austempered ductile iron by magnetic characteristics, 1991 World Conference on ADI. March 12–14, 1991. (Bloomingdale IL, pp. 6.7–7.4).
5. C. Gatelier-Rothea, J. Chicois, R. Fougeres, and P. Fleischmann, Characterization of pure iron and (130 ppm) carbon-iron binary alloy by Barkhausen noise measurements: Study of the influence of stress and microstructure, *Acta Mater* **46**, pp. 4873–4882 (1998).
6. O. Saquet, J. Chicois, and A. Vincent, Barkhausen noise from plain carbon steels: Analysis of the influence of microstructure, *Mater. Sci. Eng.* **A269**, pp. 73–82 (1999).
7. V. Moorthy, S. Vaidyanathan, Baldev Raj, T. Jayakumar, and B. P. Kashayp, Insight into the microstructural characterization of ferritic steels using micromagnetic parameters. *Metall. Mat. Trans. A* **31A**, pp. 1053–1065 (2000).
8. A. Trudel and M. Gagné, Effect of composition and heat treatment parameters on the characteristics of austempered ductile irons, *Can. Metall. Q.* **36**, pp. 289–298 (1997).
9. T. N. Rouns and K. B. Rundman, Constitution of austempered ductile iron and kinetics of austempering, *AFS Trans.* pp. 851–874 (1987).
10. Chikazumi, *Physics of Ferromagnetism* (Clarendon Press, Oxford, 1997).
11. P. Cizeau, S. Zapperi, G. Durin, and E. Stanley, Dynamics of a ferromagnetic domain wall and the Barkhausen effect, *Phys. Rev. Lett.* **79**, pp. 4669–4672 (1997).
12. J. Yi, B. Lee, and H. C. Kim, Non destructive evaluation of isothermally annealed 12% CrMoV steel by magnetic BN measurement, *J. Magnetism Magnet. Mater.*, **130**, pp. 81–91 (1994).
13. R. Ranjan, D. C. Jiles, and P. K. Rastogi, Magnetic properties of decarburized steels: An investigation of the effects of grain size and carbon content, *IEEE Trans. Magnet.* **23**, pp. 1869–1876 (1987).
14. D. J. Buttle, C. B. Scruby, G. A. D. Briggs, and J. P. Jakubovics, The measurements of stress by magnetoacoustic and Barkhausen emission, *Proc. Royal Soc. Lond.* **A414**, pp. 469–497 (1987).
15. J. Chicois and D. Tapuleasa, Qualitative considerations concerning stress characterization by various micro-magnetic techniques, *Proc. COFREND Congr. NDT*, pp. 607–613 (1997).
16. C. D'Amato, Non Destructive Characterization of Austempered Ductile Iron, Ph.D. thesis, INSA de Lyon (in preparation).

17. A. Kutsov, Y. Taran, K. Uzlov, A. Krimmel, and E. Evsyukov, Formation of bainite in ductile iron, *Mater. Sci. Eng.* **A273–275**, pp. 480–484 (1999).
18. M. G. Hetherington, and J. P. Jakubovics, High-voltage electron microscopy studies of domain-structures and magnetization processes in pearlitic steels, *Phil. Mag. B* **56**, pp. 561–577 (1987).
19. O. Saquet, D. Tapuleasa, and J. Chicois, Use of Barkhausen noise for determination of surface hardened depth, *Nondestruct. Test. Eval.* **14**, pp. 277–292 (1998).
20. G. Bach, K. Goebbels, and W. A. Theiner, Characterization of hardening depth by Barkhausen noise measurement, *Materials Evaluation*, November, pp. 1576–1580 (1988).
21. J. Kameda, Characterization of tempered martensite microstructure and embrittlement by acoustic and magnetic Barkhausen signal measurement, *Scripta Metall.* **22**, pp. 1487–1491 (1988).
22. M. Celasco and F. Fiorillo, The effect of surface on the power spectrum of the Barkhausen noise in ferromagnetic materials, *IEEE Trans. Magnet.* **10**, pp. 115–117 (1974).